Auroral spirals at Saturn

A. Radioti,[1] D. Grodent,[1] J.-C. Gérard,[1] E. Roussos,[2] D. Mitchell,[3] B. Bonfond[1] and W. Pryor[4]

A. Radioti, Laboratoire de Physique Atmosphérique et Planétaire, Institut d'Astrophysique et de Géophysique, Université de Liège, Belgium. (a.radioti@ulg.ac.be)

[1]Laboratoire de Physique Atmosphérique et Planétaire, Institut d'Astrophysique et de Géophysique, Université de Liège, Belgium

[2]Max-Planck-Institute for Solar System Research, Goettingen, Germany

[3]Applied Physics Laboratory, Johns Hopkins University, Laurel, Maryland, USA

[4]Science Department, Central Arizona College, Coolidge, Arizona, USA

Abstract.

We report observations of auroral spirals at Saturn propagating from midnight to noon via dawn, based on Cassini/UVIS measurements. The aurora during that sequence is observed for the first time to consist of detached features swirling as they propagate from dawn to early afternoon. The features have a diameter of ∼6000 km in the ionosphere, which would correspond to 12 to 15 R_S -wide plasma regions in the magnetosphere. Simultaneous ENA enhancements are observed, however, they do not show a clear spiral form. We estimate the velocity of the UV auroral features to decrease from 85% of rigid corotation (28°/h) near the equatorward edge to 68% of rigid corotation (22°/h) in the poleward edge. We discuss two posible scenarios which could explain the generation of the auroral spirals. Firstly, we suggest that the auroral spirals could be related to large dynamic hot populations which create regions with strong velocity gradients. Alternatively, a less possible theory could be that the auroral spirals are related to field line deformation from the magnetosphere to the ionosphere, similar to the scenario proposed to explain auroral spirals at Earth. Such field line twist can happen for a configuration where the magnetospheric source region is located between a pair of plasma flow vortices.

1. Introduction

Several theoretical and observational studies have dealt with the complexity of the auroral morphology at Saturn. Early studies suggested that the brightness and shape of Saturn's aurora varies with time and its general morphology corresponds to solar wind changes [*Grodent et al.*, 2005; *Clarke et al.*, 2009]. Simultaneous HST and Cassini observations suggested that the quasi-continuous main UV emission at Saturn is produced by magnetosphere-solar wind interaction, through the shear in rotational flow across the open closed field line boundary [*Bunce et al.*, 2008]. Magnetic reconnection in the dayside magnetopause as well as in the nightside tail are suggested to largely influence the morphology of Saturn's aurora [*Cowley et al.*, 2004; *Badman et al.*, 2005].

The UV dawn auroral region, which is the main focus of the current study, is occasionally observed to exhibit bright enhancements and poleward auroral expansions often accompanied by closure of open magnetic flux [*Mitchell et al.*, 2009; *Nichols et al.*, 2014; *Radioti et al.*, 2014, 2015; *Badman et al.*, 2015]. Such bright enhancements in the dawn sector are often attributed to nightside reconnection events. Small-scale intensifications in the nightside auroral emission are suggested to be signatures of dipolarisation in the tail [*Jackman et al.*, 2013] and the precursor to a more intense activity following tail reconnection [*Mitchell et al.*, 2009]. Localised UV enhancements related to tail reconnection are observed to evolve into arc and spot-like small scale features, which resemble spirals [*Radioti et al.*, 2015]. These features are suggested to be related to plasma flows enhanced from reconnection which diverge into multiple narrow channels then spread azimuthally and radially. Additionally, small scale structures (from 500 km to several thousands of km) are observed by UVIS at 06 to 18 LT and are related to patterns of upward field aligned currents related to Kelvin-Helmholtz instabilities in the magnetopause of Saturn [*Grodent et al.*, 2011]. Plasma vortices associated to Kelvin-Helmholtz instability are observed in Saturn's dawn magnetopause and are suggested to form field-aligned current systems which give rise to vortex footprints in the ionosphere [*Fukazawa et al.*, 2007; *Masters et al.*, 2010]. Finally, *Meredith et al.* [2013] reported detached small-scale structures in Saturn's prenoon UV aurora, based on Hubble Space Telescope observations, and interpreted them as signatures of field-aligned currents associated with propagating ULF waves.

In this study we investigate the origin of large spiral auroral features in the dawn sector and in one possible interpretation we consider their association with particle injections. A multi-instrumental study which combined UV, ENA (Energetic Neutral Atoms) and SKR emissions [*Mitchell et al.*, 2009] showed that UV auroral enhancements in the dawn sector are indicative of the initiation of several recurrent acceleration events in the midnight to dawn quadrant at radial distances of 15-20 R_S. Saturn's magnetospheric injections are associated with inward moving flux tubes related to interchange instability (e.g. *Mauk et al.* [2005]; *Paranicas et al.* [2007]) or particle acceleration related to the collapse of the plasma sheet and tail reconnection (e.g. [*Carbary et al.*, 2008; *Mitchell et al.*, 2009]). Both types of injections are investigated based on energetic particles and ENA emissions and are believed to be connected with each other [*Mitchell et al.*, 2014a]. Particle injections have been previously suggested to generate auroral emissions at Saturn [*Radioti et al.*, 2009, 2013b]. Pitch angle diffusion and electron scattering within the injection region as well as field-aligned currents driven by the pressure gradients along the boundaries of the injected hot plasma cloud could generate aurora.

2. Observations of auroral spirals at Saturn

Figure 1 shows a sequence of polar projections of Saturn's southern hemisphere obtained with the FUV channel (111-191 nm) of the UVIS instrument [*Esposito et al.*, 2004] on board Cassini on DOY 197, 2008. The projections are constructed by combining slit scans, which provide 64 spatial pixels of 1 mrad (along the slit) by 1.5 mrad (across the slit) and the emission is assumed to peak at an altitude of 1100 km, using the method described by *Grodent et al.* [2011]. Between the start of the 1st image and the end of the last image, the sub-spacecraft planetocentric latitude increased from -28.7 to -21.4 degrees and the spacecraft altitude changed from 9.5 to 11.5 R_S. Because of the relatively high sub-spacecraft latitude, the limb brightening effect is limited and therefore no correction was applied.

During this sequence the main emission in the dawn sector consists of three detached features labelled with a, b and c in Figure 1. The features are initially observed to be aligned with the main emission, while as they propagate towards noon they form spirals, a shape that is less evident for feature c. It should be noted that even though the features do not completely satisfy the definition of a spiral, as they do not seem to curve out from a central point, in the following we keep on using the term 'spiral' for simplicity. A close up view of the auroral features a and b is presented in Figure 2. We choose to analyse further only features a and b as their spiral shape is more evident in the UVIS images. Particularly, in the first five panels (up to 0638 UT) the features are not very well organised. They are observed to be aligned with the main emission, while progressively their shape changes and they become wider. The leading edge is moving slightly poleward and the trailing edge is moving equatoward, an evolution more evident for feature b. At 0638 UT the features take a circular and coherent form. Two circles are drawn on top of the emissions in the panel at 0638 UT for guidance. The spiral pattern continues during at least the first half of the sequence (until 0800 UT). Afterwards the leading part of the emissions is mainly evident, while the trailing part is fainter. A movie constructed based on the polar projections of Figure 1 is included in the auxiliary material and shows the evolution and motion of the features. The diameter of the features in the ionosphere is on the order of 6000 km. The auroral features correspond to 12 to 15 R_S -wide plasma regions in the magnetosphere. For the magnetic mapping on the equatorial plane we use a magnetic field model incorporating a current sheet with half thickness of 2.5 R_S, a magnetopause standoff distance of 22 and 27 R_S, consistent with *Achilleos et al.* [2008] inner and outer magnetopause boundary position, and the current sheet scaling laws from *Bunce et al.* [2007]. The 'Cassini' model of *Dougherty et al.* [2005] is used as internal magnetic field model.

Even though the morphology of this auroral region has been occasionally observed to change drastically (dramatic brightness enhancements and poleward expansions [*Mitchell et al.*, 2009; *Nichols et al.*, 2014; *Radioti et al.*, 2014, 2015; *Badman et al.*, 2015]), this is the first time that it is observed to break into separate detached spiral features along a large local time sector (8 hours in LT). It should be noted that *Meredith et al.* [2013] recently reported detached small-scale UV structures between 05 and 11 LT, which however do not exhibit a spiral form. UV features which resemble small-scale spirals are recently observed at one snapshot and were related to plasma flows enhanced from tail reconnection [*Radioti et al.*, 2015].

The emissions discussed here should not be confused with the 'bifurcations' of the main emission at noon-dusk quadrant [*Radioti et al.*, 2011, 2013a], even though at the later stage of their development (panel at 0950 and 1018 UT of Figure 1), they resemble morphologically the bifurcations. The UV spirals are observed to originate in the postmidnight-predawn sector, while the auroral bifurcations are generated at noon (see Figure 1 in [*Radioti et al.*, 2011]). The later are interpreted as magnetopause reconnection signatures based on their observed location and on the expansion of the main emission to lower latitudes following the appearance of the bifurcations [*Radioti et al.*, 2011].

Simultaneously with the UV observations, the ion and neutral camera (INCA) on board Cassini observed a localized enhancement in ENA emissions from Saturn's magnetosphere, evidence of a rotating heated plasma region whose peak emission is located near 7-10 R_S in the dawn-noon quadrant, possibly related to magnetospheric injections. Figure 3 shows the ENA enhancement (indicated by the yellow arrow on the first panel) which starts in the midnight-dawn quadrant (0200 UT), passes through dawn and then goes out of the field of view. The images are integrated during 40 minutes centered on the time indicated and the x-axis points noon. Due to the orientation of the camera a part of the emission moves out of the field of view after 08:00 UT. The ENA emissions here consist of several substructures. However, it is unclear whether they exhibit spiral forms, as we cannot resolve the detailed structure due to limited resolution. Comparison of the UVIS and INCA measurements suggests that the ENA enhancement is observed simultaneously and on the same location as the UV feature a and partially b (Figure 1), implying that both

UV and ENA emissions are associated with the same dynamical event. Previous studies showed that similar ENA enhancements are closely correlated with UV transient features and are related to the same energetic particle injection event [*Mitchell et al.*, 2009; *Radioti et al.*, 2013b].

3. On the origin of the auroral spirals

3.1. Large scale energetic particle injections

The UV auroral spirals observed here might be the optical signatures of large magnetospheric particle injections extended over several R_S. Saturn's magnetosphere contains several sources of heated plasma either associated with inward moving flux tubes related to interchange instability or particle acceleration related to nightside reconnection [*Mitchell et al.*, 2014a]. An association of the present UV auroral emissions with magnetospheric injections is supported by the simultaneous UV-ENA emissions as discussed above. Additionally, the UV brightness of the features decays with time, which is in accordance with the expectations of the UV counterpart of particle injections, considering pitch angle diffusion and electron scattering as the driving mechanism [*Radioti et al.*, 2013b]. However, it should be noted that this cannot be the only triggering mechanism, as field-aligned currents driven by the pressure gradients along the boundaries of the injected hot plasma cloud related to the ENA enhancements should contribute to the UV emission part, as explained by *Radioti et al.* [2013b].

A key parameter responsible for the spiral shape of the auroral emission is the corotation lag of the source population. Within an injection event the corotation fraction might change locally, because of the dynamics of the feature. *Carbary and Mitchell* [2014] analysed ENA measurements and revealed substructures within the ENA emissions and large velocity variations as a function of local time and L-shell. They showed that in the dawn sector the velocities decrease with radial distance (with an exception of a local increase of the velocities at 20 R_S). In particularly, they showed that the velocity may vary in the dawn sector from $\sim$30°/h ($\sim$90% of rigid corotation) at 5 R_S to $\sim$23°/h ($\sim$68% of rigid corotation) at 20R_S. In addition to ENA emissions, particle measurements have been used to investigate the flow velocities. *Thomsen et al.* [2010] showed that the measured azimuthal flow speeds are characteristically below full corotation over 5 to 20 L-Shell, varying on average from $\sim$50% to $\sim$70% of rigid corotation. *Livi et al.* [2014] demonstrated that between 10 and 13 R_S the thermal plasma rotation velocity accelerates once more toward rigid corotation but abruptly stops at 13 R_S. They also showed that the velocities may vary largely at given radial distance. For example at 12 R_S it may vary from 20 to 80% of rigid corotation.

In the following, we estimate the velocity of the auroral feature based on the present observations. We trace the motion of the feature a starting from panel at 0611 UT, as in the beginning of the sequence the emission changes randomly from panel to panel and at around 0611 UT stabilises its shape. We follow the motion of the leading part of the emission (leading in local time) which persists until the end of the sequence. We trace the longitude of the peak of the emission at certain latitudes (70°, 71°, 72°, 73° and 74°) and plot it as a function of time (panel a Figure 4). These locations are shown by the yellow diamonds on top of the emission at panels 0706 and 0855 UT of Figure 2. We apply a linear fit function (solid lines in panel a of Figure 4) to the set of data at each latitude and we show that the emission rotates at a different fraction of the rigid corotation starting from 68% (22°/h) for the poleward part and increasing up to 85% (28°/h) for the most equatorward part. In our analysis we consider that the electron drift is only due to corotation, because the gradient-curvature drift is negligible at these L-Shells. This statement is based on the estimation of the gradient-curvature drift for electron energies between 1-10 KeV, which we find to be on the order of 5% of the corotation for the L-shell under study, following the method described in *Roussos et al.* [2013].

Panel b Figure 4 shows the decrease of the feature's corotation fraction as a function of latitude. The magnetically mapped radial distance is also indicated. The corotation fraction is estimated to decrease with a rate of 4.2% of rigid corotation per degree of latitude based on a linear fit (solid line). In Figure 4, panel c we plot a simulated emission as a function of time based on the estimated corotation fraction. The snapshots are calculated every 50 minutes and each color stands for the emission at different latitudes. The simulated pattern resembles the motion of the leading part of the observed auroral spiral. It should be noted that here we consider only the leading part of the auroral emission. The evolution of the trailing part (lagging in local time) also requires a velocity gradient. However, a similar analysis for the trailing part, which aims to derive the gradient, would be inaccurate due to the fact that the spiral shape is not conserved until the end of the sequence, possibly because the emission is below the UVIS threshold.

We suggest that the spiral auroral features could be the ionospheric signatures of large (12-15 R_S) injections, considering that within the injection the corotation fraction changes locally, because of the dynamical behaviour of the event. This scenario could work for strong velocity gradients at a rate of 4.2 % of rigid corotation per degree of latitude, as it is shown in the above analyses. The velocities estimated from the auroral measurements, which result at the velocity gradient are in accordance with the particle velocities derived based on magnetospheric data [*Thomsen et al.*, 2010; *Livi et al.*, 2014] and ENA emissions [*Carbary and Mitchell*, 2014].

3.2. Field line deformation from the magnetosphere to the ionosphere

Another possible interpretation of the UV auroral spirals, indirectly related to magnetospheric plasma vortices, is field line deformation (twist) from the magnetosphere to the ionosphere as suggested to explain auroral spirals (of 200-300 km large) at Earth [*Keiling et al.*, 2009] and illustrated in panel a, Figure 5. Field line deformation can happen for a configuration where the magnetospheric source region is located between a pair of opposite rotating plasma flow vortices. The auroral spiral is related to a magnetic field-aligned current system which is generated to connect the magnetospheric source region with the ionosphere [*Keiling et al.*, 2009]. This scenario is in accordance with the fact that the magnetospheric ENA emissions (Figure 3) do not form clear spirals, while the simultaneous UV emissions (Figure 1) at the polar end of the twisted field lines form spiral structures. The field line deformation theory differs from the scenario related to injections. According to it, the spiral shape of the auroral emission is the result of the twist of the field lines from the magnetosphere to the ionosphere and does not require an extended in latitude (radial distance) magnetospheric plasma population with strong velocity gradient, as it is the case for the scenario related to injections.

A similar process is suggested to explain auroral spiral-like structures observed only during a snapshot, following the onset of tail reconnection [*Radioti et al.*, 2015]. The present observations differ from those reported in *Radioti et al.* [2015], as they describe large scale spirals that are persistent for several hours. The formation of the spirals observed here could be related to vortices not necessary associated with tail reconnection.

The field line deformation scenario requires that the auroral spiral is not the ionospheric footprint of the magnetospheric plasma flow vortex, but however, flow vortices are essential for providing the necessary conditions for the generation process of the auroral spiral form. Cassini's energetic particle detector observed fast and brief episodes of convective flows in the nightside magnetosphere [*Mitchell et al.*, 2014a], which have been identified as transitional events between current sheet collapse and interchange. The brief periods of radial flow could set up oppositely directed flow at their boundaries, assuming they are limited in azimuth. Additionally, simulation studies [*Jia et al.*, 2012] predict fast plasma flows, released from tail reconnection at Saturn, to move towards the planet and create flow shear with the surroundings. Consequently, those rapidly moving flux tubes are expected to generate strong disturbances in the ionosphere. Plasma vortices in the Saturnian magnetosphere could be formed by nonlinear Kelvin-Helmholtz instabilities at Saturn's morning magnetopause [*Masters et al.*, 2010]. However, such vortices cannot provide the necessary conditions for the spiral formation in the ionosphere, in the context of the field-line deformation scenario, as a pair of them would be same-directed.

In summary, even though there are arguments that a field line deformation theory could form auroral spirals at Saturn, this might not be the most possible scenario to interpret the present observations. The main concern is that there is no direct evidence that a twin vortex in the equatorial plane could remain coherent with time over a large local time sector, in order to support the persistence of the spiral shape observed here over several hours.

4. Summary and conclusions

In this study we report for the first time auroral spirals at Saturn propagating from midnight to noon. The emission consists of several persistent detached swirling features extended over a larger local time sector. Simultaneously ENA enhancements are observed, however, they do not show a clear vortical form, possibly due to their limited resolution. The UV features have a diameter of ∼6000 km in the ionosphere, which would correspond to 12 to 15 R_S -wide plasma regions in the magnetosphere. We estimated the velocity of the auroral feature and concluded that there is a strong velocity gradient with a decrease rate of 4.2% of rigid corotation per degree of latitude. In particularly, we show that the velocity decreases from 85% (28°/h) in the equatorward part to 68% (22°/h) in the poleward part. Particle velocities derived from magnetospheric data [*Thomsen et al.*, 2010; *Livi et al.*, 2014] and ENA emissions [*Carbary and Mitchell*, 2014], showed large variations of the corotation velocity fraction as a function of radial distance in accordance with the values derived from the auroral observations. We discuss two scenarios as possible mechanisms for the generation of the auroral spirals.

Firstly, we suggest that the spiral auroral features could be the ionospheric signatures of large (12-15 R_S) injections, considering that within the injection the corotation fraction changes locally, because of the dynamical behaviour of the event. We perform a simple simulation of the auroral emission considering magnetospheric plasma regions rotating at different velocities and we generate the observed auroral pattern. This scenario could work for strong velocity gradients at a rate of 4.2 % of rigid corotation per degree of latitude. Alternatively, we consider field line deformation (twist) from the magnetosphere to the ionosphere, illustrated in panel a, Figure 5, as another possible mechanism that could generate the auroral spirals. According to this scenario the auroral spiral is not the ionospheric footprint of the magnetospheric plasma flow vortex, but flow vortices are essential for providing the necessary conditions for the generation process of the auroral spiral form. This scenario is in accordance with the fact that the magnetospheric ENA (Figure 3) emissions do not form clear spirals, while the simultaneous UV emissions (Figure 1) at the polar end of the twisted field lines form spiral structures. This is however, a less possible theory as there is not evidence that a twin vortex in the equatorial plane could remain coherent with time over a large local time sector. Finally, it should be noted that the auroral features observed here could not be the direct optical signatures of plasma vortical flows related to Kelvin-Helmholtz instabilities in the magnetopause [*Masters et al.*, 2010]. The Kelvin-Helmholtz vortical flows are generated close to noon and propagate antisunward, while the UV features here are detected in the pre-dawn sector and propagate with a large velocity of 68 to 85 % of rigid corotation towards noon.

Acknowledgments.

This work is based on observations acquired with the UVIS instrument onboard the NASA/ESA Cassini spacecraft and are available in https://pds.jpl.nasa.gov/tools/subscription_service/SS-20150703.shtml. This research was supported by the Belgian Fund for Scientific Research (FNRS) and the PRODEX Program managed by the European Space Agency in collaboration with the Belgian Federal Science Policy Office. B.B. is funded by the Belgian Fund for Scientific Research (FNRS).

References

Achilleos, N., C. S. Arridge, C. Bertucci, C. M. Jackman, M. K. Dougherty, K. K. Khurana, and C. T. Russell, Large-scale dynamics of Saturn's magnetopause: Observations by Cassini, *Journal of Geophysical Research (Space Physics)*, *113*, 11,209, 2008.

Badman, S. V., E. J. Bunce, J. T. Clarke, S. W. H. Cowley, J.-C. GéRard, D. Grodent, and S. E. Milan, Open flux estimates in Saturn's magnetosphere during the January 2004 Cassini-HST campaign, and implications for reconnection rates, *Journal of Geophysical Research (Space Physics)*, *110*, 11,216, 2005.

Badman, S. V., et al., Saturns auroral morphology and field-aligned currents during a solar wind compression, *Icarus*, 2015.

Bunce, E. J., S. W. H. Cowley, I. I. Alexeev, C. S. Arridge, M. K. Dougherty, J. D. Nichols, and C. T. Russell, Cassini observations of the variation of Saturn's ring current parameters with system size, *Journal of Geophysical Research (Space Physics)*, *112*, 10,202, 2007.

Bunce, E. J., et al., Origin of Saturn's aurora: Simultaneous observations by Cassini and the Hubble Space Telescope, *Journal of Geophysical Research (Space Physics)*, *113*, 9209, 2008.

Carbary, J. F., and D. G. Mitchell, Keogram analysis of ENA images at Saturn, *Journal of Geophysical Research (Space Physics)*, *119*, 1771–1780, 2014.

Carbary, J. F., D. G. Mitchell, P. Brandt, E. C. Roelof, and S. M. Krimigis, Statistical morphology of ENA emissions at Saturn, *Journal of Geophysical Research (Space Physics)*, *113*, 5210, 2008.

Clarke, J. T., et al., Response of Jupiter's and Saturn's auroral activity to the solar wind, *Journal of Geophysical Research (Space Physics)*, *114*, 5210, 2009.

Cowley, S., E. Bunce, and R. Prangé, Saturn's polar ionospheric flows and their relation to the main auroral oval, *Annales Geophysicae*, *22*, 1379–1394, 2004.

Dougherty, M. K., et al., Cassini Magnetometer Observations During Saturn Orbit Insertion, *Science*, *307*, 1266–1270, 2005.

Esposito, L. W., et al., The Cassini Ultraviolet Imaging Spectrograph Investigation, *Space Science Review*, *115*, 299–361, 2004.

Fukazawa, K., T. Ogino, and R. J. Walker, Vortex-associated reconnection for northward IMF in the Kronian magnetosphere, *Geophys. Res. Lett.*, , *34*, 23,201, 2007.

Grodent, D., J.-C. Gérard, S. W. H. Cowley, E. J. Bunce, and J. T. Clarke, Variable morphology of Saturn's southern ultraviolet aurora, *Journal of Geophysical Research (Space Physics)*, *110*, 7215, 2005.

Grodent, D., J. Gustin, J.-C. Gérard, A. Radioti, B. Bonfond, and W. R. Pryor, Small-scale structures in Saturn's ultraviolet aurora, *Journal of Geophysical Research (Space Physics)*, *116*, 9225, 2011.

Jackman, C. M., N. Achilleos, S. W. H. Cowley, E. J. Bunce, A. Radioti, D. Grodent, S. V. Badman, M. K. Dougherty, and W. Pryor, Auroral counterpart of magnetic field dipolarizations in Saturn's tail, *Planetary and Space Science*, *82*, 34–42, 2013.

Jia, X., K. C. Hansen, T. I. Gombosi, M. G. Kivelson, G. Tóth, D. L. DeZeeuw, and A. J. Ridley, Magnetospheric configuration and dynamics of Saturn's magnetosphere: A global MHD simulation, *Journal of Geophysical Research (Space Physics)*, *117*, 5225, 2012.

Keiling, A., et al., THEMIS ground-space observations during the development of auroral spirals, *Annales Geophysicae*, *27*, 4317–4332, 2009.

Livi, R., J. Goldstein, J. L. Burch, F. Crary, A. M. Rymer, D. G. Mitchell, and A. M. Persoon, Multi-instrument analysis of plasma parameters in Saturn's equatorial, inner magnetosphere using corrections for corrections for spacecraft potential and penetrating background radiation, *Journal of Geophysical Research (Space Physics)*, *119*, 3683–3707, 2014.

Masters, A., et al., Cassini observations of a Kelvin-Helmholtz vortex in Saturn's outer magnetosphere, *Journal of Geophysical Research (Space Physics)*, *115*, 7225, 2010.

Mauk, B. H., et al., Energetic particle injections in Saturn's magnetosphere, *Geophys. Res. Lett.,* , *32*, 14, 2005.

Meredith, C. J., S. W. H. Cowley, K. C. Hansen, J. D. Nichols, and T. K. Yeoman, Simultaneous conjugate observations of small-scale structures in Saturn's dayside ultraviolet auroras: Implications for physical origins, *Journal of Geophysical Research (Space Physics)*, *118*, 2244–2266, 2013.

Mitchell, D. G., et al., Recurrent energization of plasma in the midnight-to-dawn quadrant of Saturn's magnetosphere, and its relationship to auroral UV and radio emissions, *Planetary and Space Science*, *57*, 1732–1742, 2009.

Mitchell, D. G., et al., Injection, Interchange, and Reconnection: Energetic Particle Observations in Saturns Magnetosphere, *Magnetotail in the Solar System, Geophysical Monograph*, 2014a.

Nichols, J. D., et al., Dynamic auroral storms on Saturn as observed by the Hubble Space Telescope, *Geophysical Research Letters*, *41*, 3323–3330, 2014.

Paranicas, C., et al., Energetic electrons injected into Saturn's neutral gas cloud, *Geophys.*

Res. Lett., , *34*, 2109, 2007.

Radioti, A., D. Grodent, J.-C. Gérard, S. E. Milan, B. Bonfond, J. Gustin, and W. Pryor, Bifurcations of the main auroral ring at Saturn: ionospheric signatures of consecutive reconnection events at the magnetopause, *Journal of Geophysical Research (Space Physics)*, *116*, 11,209, 2011.

Radioti, A., D. Grodent, J.-C. Gérard, B. Bonfond, J. Gustin, W. Pryor, J. M. Jasinski, and C. S. Arridge, Auroral signatures of multiple magnetopause reconnection at Saturn, *Geophysical Research Letters*, *40*, 4498–4502, 2013a.

Radioti, A., E. Roussos, D. Grodent, J.-C. GéRard, N. Krupp, D. G. Mitchell, J. Gustin, B. Bonfond, and W. Pryor, Signatures of magnetospheric injections in Saturn's aurora, *Journal of Geophysical Research (Space Physics)*, *118*, 1922–1933, 2013b.

Radioti, A., D. Grodent, J.-C. Gérard, S. E. Milan, R. C. Fear, C. M. Jackman, B. Bonfond, and W. Pryor, Saturn's elusive nightside polar arc, *Geophysical Research Letters*, 2014.

Radioti, A., D. Grodent, X. Jia, J. C. Gérard, B. Bonfond, W. Pryor, J. Gustin, D. G. Mitchell, and C. M. Jackman, A multi-scale magnetotail reconnection event at Saturn and associated flows: Cassini/UVIS observations, *Icarus*, 2015.

Radioti, A., et al., Transient auroral features at Saturn: Signatures of energetic particle injections in the magnetosphere, *Journal of Geophysical Research (Space Physics)*, *114*, 3210, 2009.

Roussos, E., M. Andriopoulou, N. Krupp, A. Kotova, C. Paranicas, S. M. Krimigis, and D. G. Mitchell, Numerical simulation of energetic electron microsignature drifts at Saturn: Methods and applications, *Icarus*, *226*, 1595–1611, 2013.

Thomsen, M. F., D. B. Reisenfeld, D. M. Delapp, R. L. Tokar, D. T. Young, F. J. Crary, E. C. Sittler, M. A. McGraw, and J. D. Williams, Survey of ion plasma parameters in Saturn's magnetosphere, *Journal of Geophysical Research (Space Physics)*, *115*, 10,220, 2010.

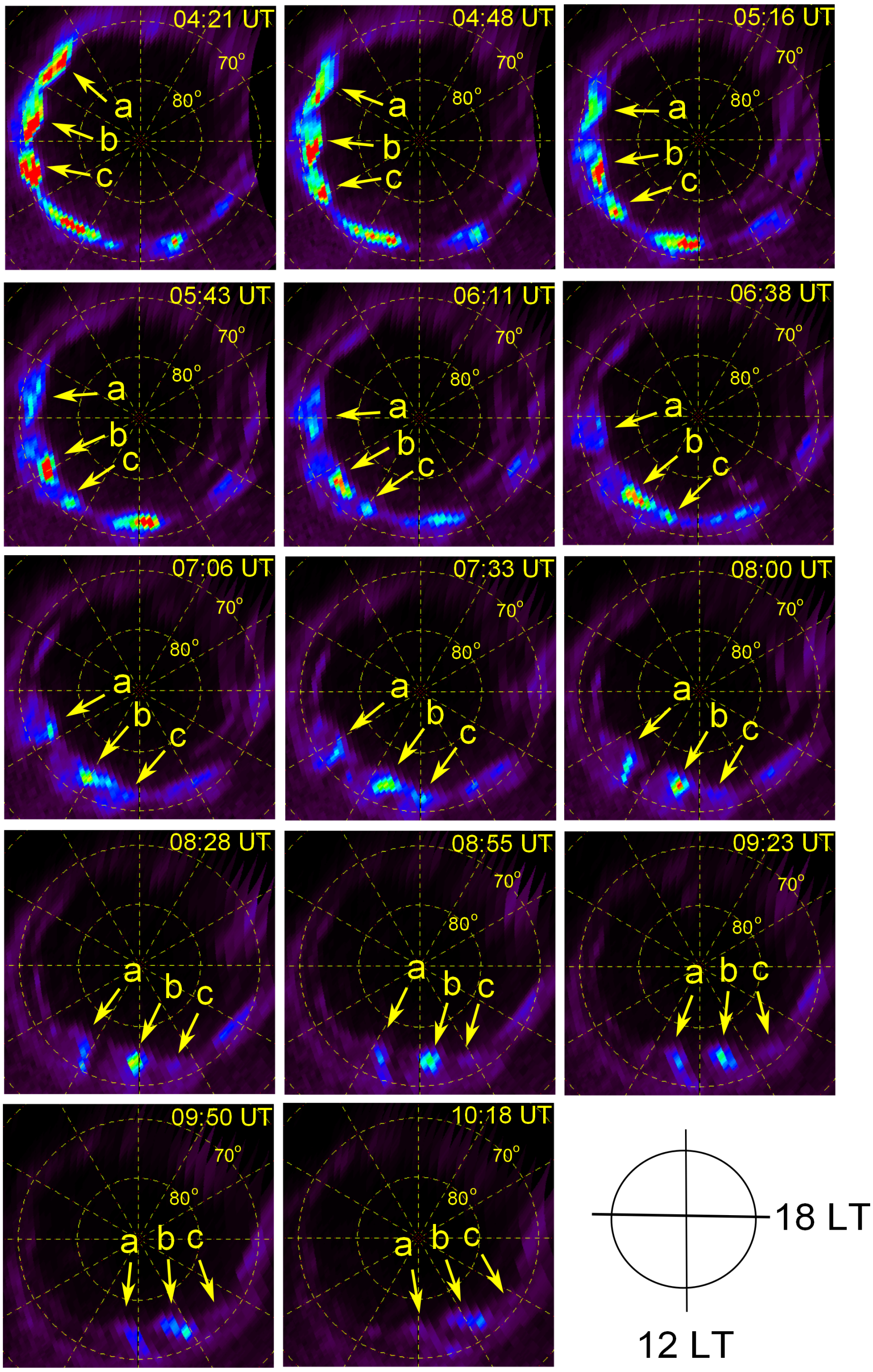

Figure 1. A sequence of polar projections of Saturn's southern aurora obtained with the FUV channel of UVIS on board Cassini. The first image starts at 0421 UT and the last one at 1018 UT on DOY 197, 2008. Noon is to the bottom and dusk to the right. The grid shows latitudes at intervals of 10° and meridians of 30°. Yellow arrows indicate the separate intensifications in the dawn-midnight quadrant. Feature a and b are exhibiting spiral structures.

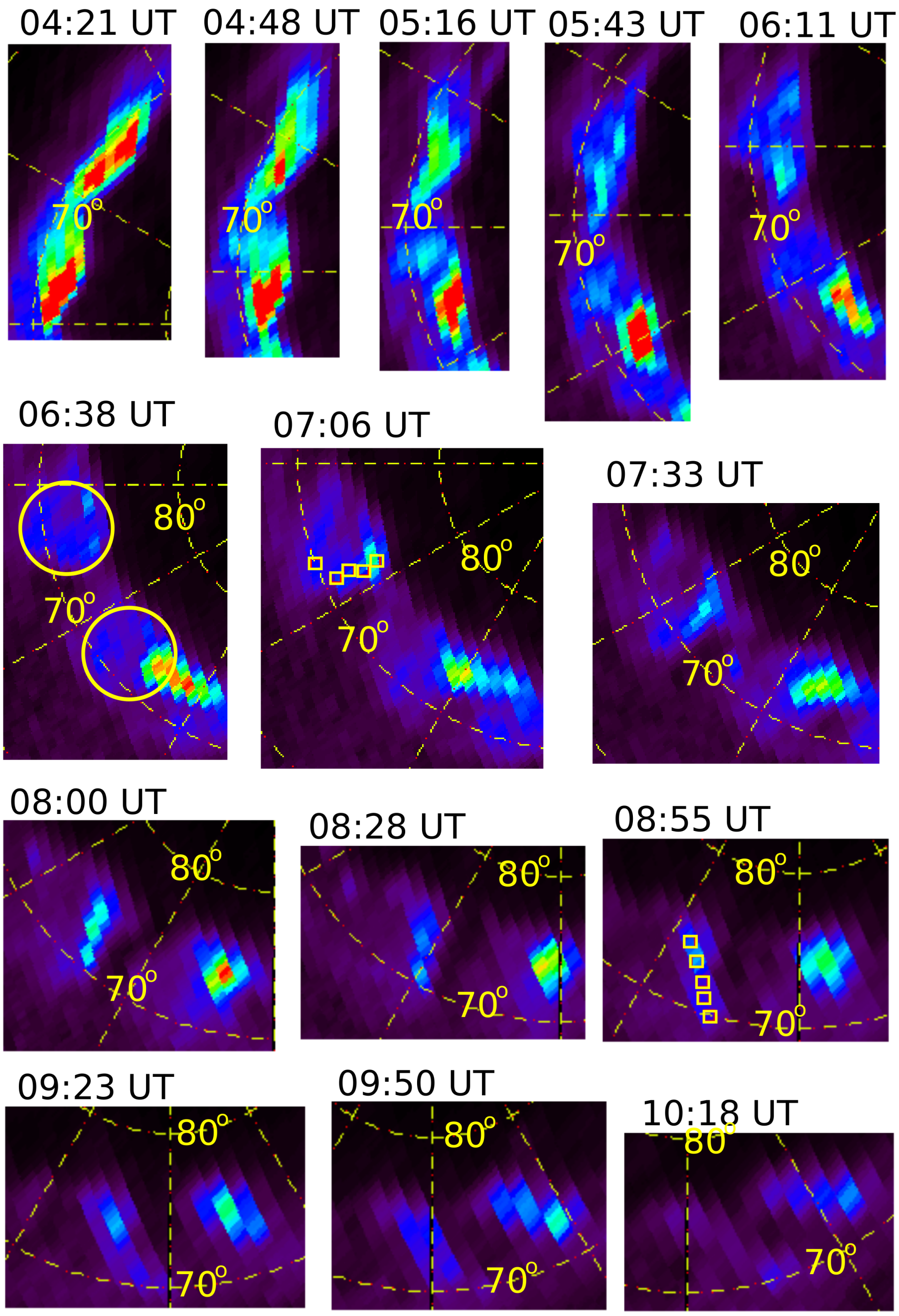

Figure 2. Projected close ups of a selected region on the polar projections from Figure 1 starting at 0421 to 1018 UT. The images show the two features a and b that form auroral spirals. Two circles are drawn on top of the two auroral features in the images taken at 0638 UT, in order to indicate the spiral form. The diamonds at panels 0706 and 0855 UT indicate the coordinates at certain latitudes (70°, 71°, 72°, 73° and 74°) used to calculate the corotation fractions.

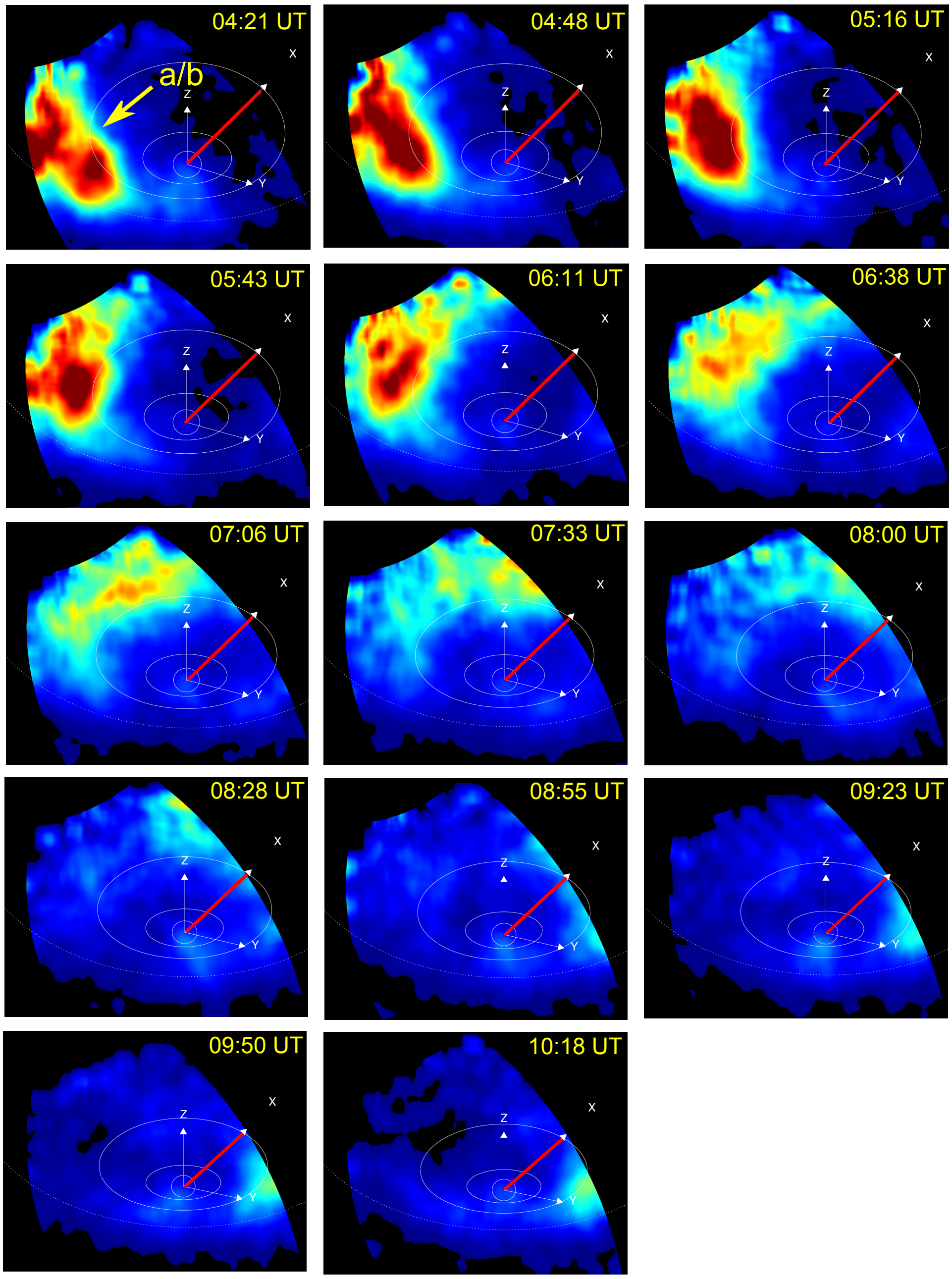

Figure 3. ENA emissions from Saturn's magnetosphere on DOY 197, 2008. The images are 40 min integration centered on the time indicated. The two circles represent the E-ring boundaries at 2.5 and 7.5 R_S. The innermost circle is Saturn's limb (1 R_S). The Z axis is aligned with Saturn's spin axis, X axis (highlighted in red) indicates the direction toward the sun, and Y axis points to dusk. Arrows indicate the ENA enhancement discussed in this work and possibly correspond to UV emission a and b shown in Figure 1.

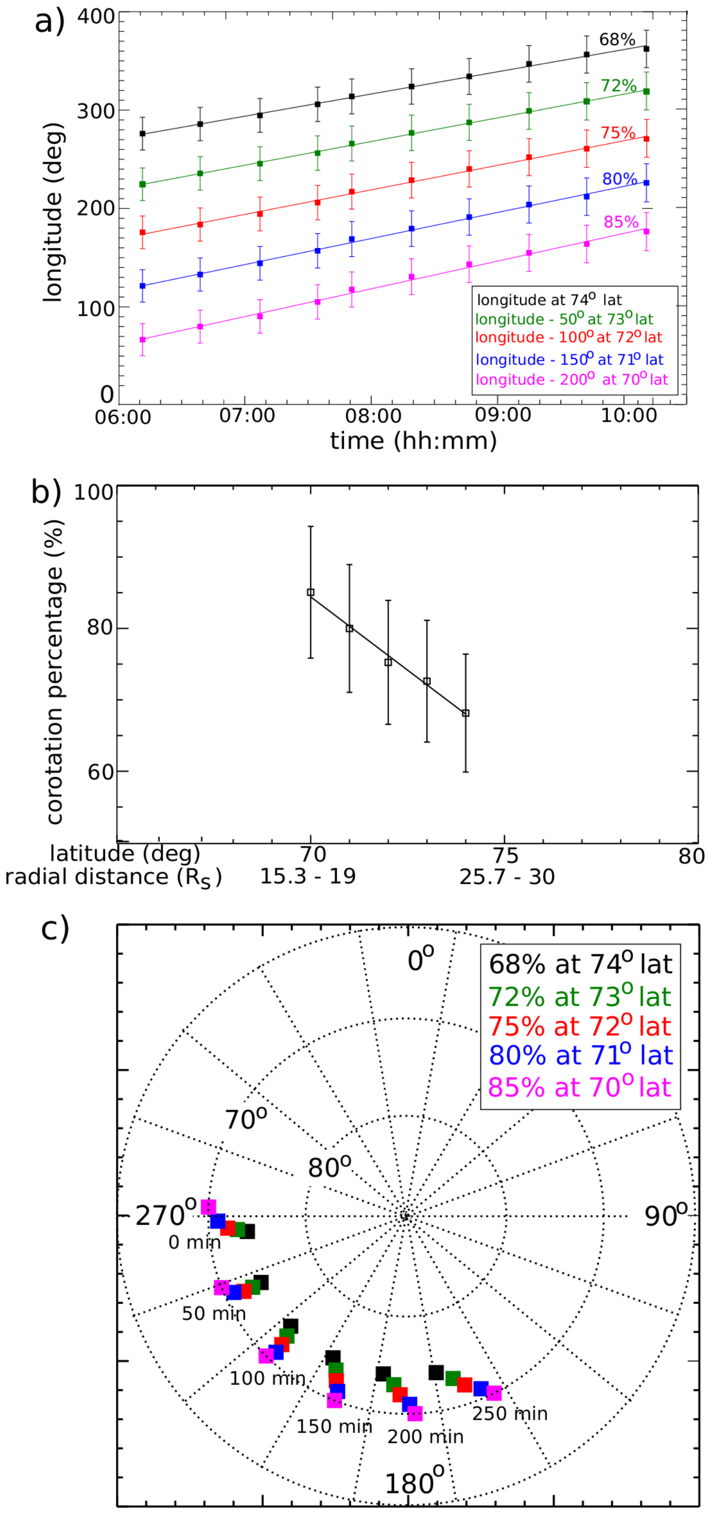
a)
longitude (deg)
time (hh:mm)
68%
72%
75%
80%
85%
longitude at 74° lat
longitude - 50° at 73° lat
longitude - 100° at 72° lat
longitude - 150° at 71° lat
longitude - 200° at 70° lat
b)
corotation percentage (%)
latitude (deg)
radial distance (R_S)
15.3 - 19
25.7 - 30
c)
68% at 74° lat
72% at 73° lat
75% at 72° lat
80% at 71° lat
85% at 70° lat
0 min
50 min
100 min
150 min
200 min
250 min

Panel a: Longitude of the leading part of the UV emission (see Figure 2) at five latitudes (70°, 71°, 72°, 73° and 74°) as a function of time. Some of these points are indicated on top of the emission at panels 0706 and 0855 UT of Figure 2. The solid lines represent a linear fit to the set of data at each latitude. The corotation rates 68%, 72%,75%,80% and 85% correspond to 22°/h, 24°/h, 25°/h, 26°/h and 28°/h, respectively. The error bars indicate the standard deviations of longitude at a given time. Panel b: shows the decrease of the feature's corotation fraction as a function of latitude. The respective magnetically mapped radial distance is derived for magnetopause standoff distance of 22 and 27 R_S and is indicated for 70° and 75° latitude. Details of the magnetic mapping are described in the text. The corotation fraction decreases at a rate of 4.2% of rigid corotation per degree of latitude based on a linear fit (solid line). Panel c: Simulated emission as a function of time based on the estimated corotation fraction. The snapshots are taken every 50 minutes and each color stands for the emission at different latitudes.

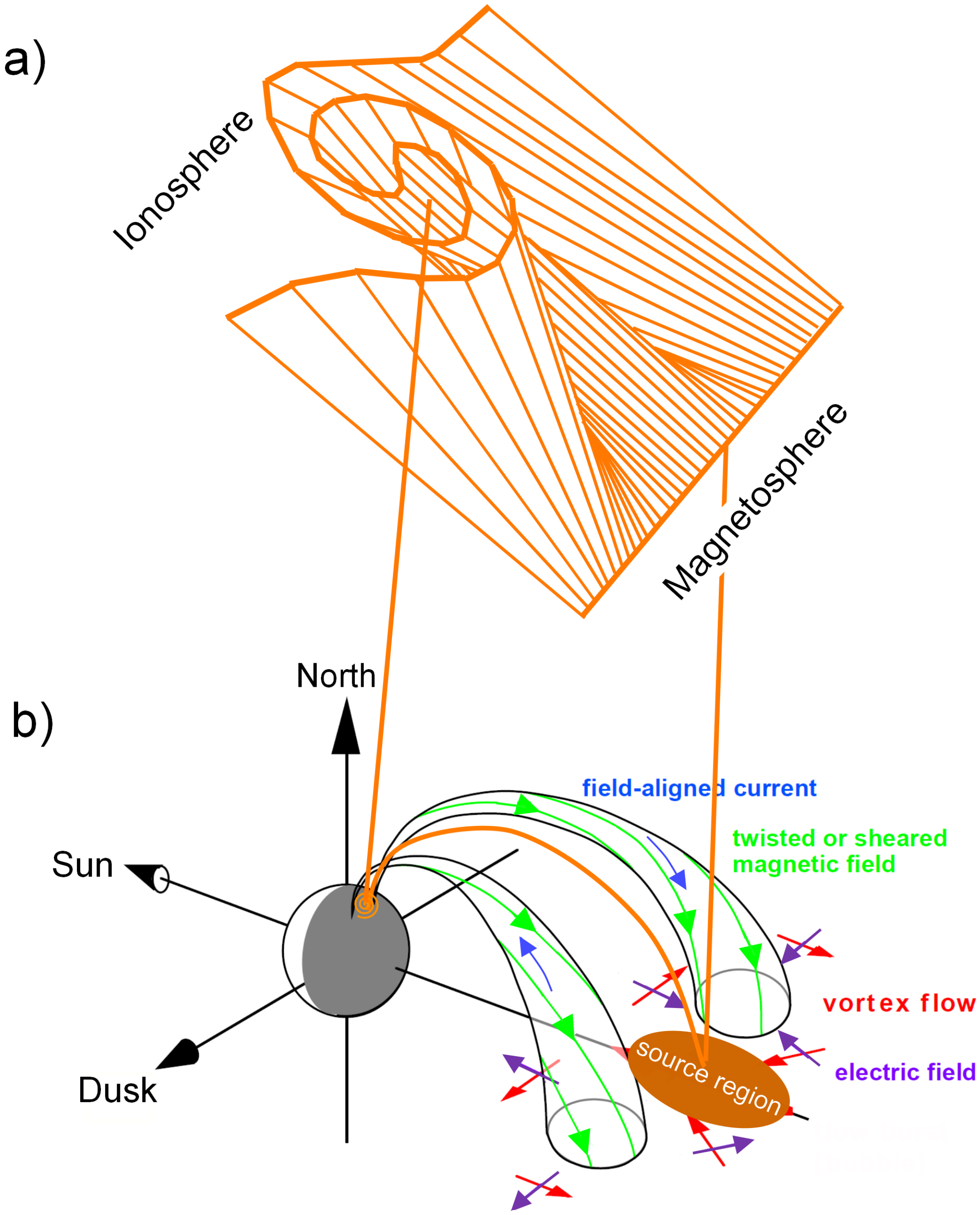

Figure 5. Schematic illustrating the generation of an auroral spiral and its source region, located between two oppositely rotating plasma vortices in the magnetosphere of Saturn (adapted from *Radioti et al.* [2015]). The field line twisting from the magnetosphere to the ionosphere, which gives rise to auroral spirals is illustrated in a close up. The same mechanism is believed to explain auroral spirals at Earth [*Keiling et al.*, 2009]. This simple illustration does not consider the bending of the field lines.